Steel and Composite Structures, Vol. 13, No. 3 (2012) 239-258
DOI: http://dx.doi.org/10.12989/scs.2012.13.3.239

Experimental investigation on flexural behaviour of HSS stud connected steel-concrete composite girders

Amar prakash*, N.Anandavalli, C.K.Madheswaran and N.Lakshmanan

CSIR- Structural Engineering Research Centre, CSIR Campus, Taramani, Chennai-600113, India

(Received December 29, 2010, Revised April 23, 2012, Accepted May 29, 2012)

Abstract. In this paper, experimental investigations on high strength steel (HSS) stud connected steel-concrete composite (SCC) girders to understand the effect of shear connector density on their flexural behaviour is presented. SCC girder specimens were designed for three different shear capacities (100%, 85%, and 70%), by varying the number of stud connectors in the shear span. Three SCC girder specimens were tested under monotonic/quasi-static loading, while three similar girder specimens were subjected to non-reversal cyclic loading under simply supported end conditions. Details of casting the specimens, experimental set-up, and method of testing, instrumentation for the measurement of deflection, interface-slip and strain are discussed. It is found that SCC girder specimen designed for full shear capacity exhibits interface slip for loads beyond 25% of the ultimate load capacity. Specimens with lesser degree of shear connection show lower values of load at initiation of slip. Very good ductility is exhibited by all the HSS stud connected SCC girder specimens. It is observed that the ultimate moment of resistance as well as ductility gets reduced for HSS stud connected SCC girder with reduction in stud shear connector density. Efficiency factor indicating the effectiveness of high strength stud connectors in resisting interface forces is estimated to be 0.8 from the analysis. Failure mode is primarily flexure with fracturing of stud connectors and characterised by flexural cracking and crushing of concrete at top in the pure bending region. Local buckling in the top flange of steel beam was also observed at the loads near to failure, which is influenced by spacing of studs and top flange thickness of rolled steel section. One of the recommendations is that the ultimate load capacity can be limited to 1.5 times the plastic moment capacity of the section such that the post peak load reduction is kept within limits. Load-deflection behaviour for monotonic tests compared well with the envelope of load-deflection curves for cyclic tests. It is concluded from the experimental investigations that use of HSS studs will reduce their numbers for given loading, which is advantageous in case of long spans. Buckling of top flange of rolled section is observed at failure stage. Provision of lips in the top flange is suggested to avoid this buckling. This is possible in case of longer spans, where normally built-up sections are used.

Keywords: steel-concrete composite girder; HSS stud connector; ductility; efficiency factor; interface slip; local buckling.

1. Introduction

Over past few decades experimental as well as analytical studies have been carried out to understand the flexural behaviour of SCC girder. Oehlers and Coughlan (1986) have derived the strength of stud shear connection in the SCC beams based on large number of push-out tests. In these types of girders,

* Corresponding author, Mr., E-mail: amar@serc.res.in

the effect of geometrical sizes and material properties of various components influences the shear interaction behaviour when subjected to flexural loading as reported by Uy and Bradford 1996, and Oehlers 1997. It has been reported by Oehlers *et al.* (1997) that if the strength of the steel section is greater than that of the concrete section then the design can become unconservative. Wang (1998) has presented the analysis for maximum deflection in steel-concrete composite beams having partial shear connection, and validated the analysis results with the experimental studies.

It is reported by Nie and Cai (2003) that even for full shear connection, the slip effects have shown 17% reduction in stiffness of short span SCC girders. Experimental study by Nie *et al.* (2004) on SCC girders with high strength concrete has shown higher initial stiffness and distinct post-yield characteristics than that with normal strength concrete. Nie *et al.* (2006) have also proposed an equivalent rigidity factor for the SCC girders containing opening in concrete flange. Jurkiewiez and Braymand (2007) have conducted experimental study on pre-cracked steel-concrete composite girders. It is reported that the failure is caused by high compressive strain and crushing of the concrete slab accompanied by plastic strains in the steel girder. Within the elastic phase, the vertical distribution of strain is linear throughout the concrete deck and the steel beam with a discontinuity at their interface. Slips at the steel-concrete interface and axial strains in the shear studs were also measured. Possibilities of realizing the adhesive bonded SCC structures have also been investigated (Bouazaaoui *et al.* 2007, Zhao and Li 2008). But, such type of shear connections in SCC girders may be vulnerable to be affected by temperature variations.

This study presents the experimental investigations carried out on six high strength (EN 19 grade steel) stud connected steel-concrete composite girders. Both quasi static/monotonic and cyclic load tests are carried out under simply supported end conditions. The SCC girder specimens are designed such that the maximum flexural capacity of the selected steel rolled beam section can be utilized upto maximum capacity. Deflections, interface slips, and strains in steel, concrete and studs are measured. The variation of the strain and deformation of embedded studs have not been investigated much in the literature. Therefore, strains are also measured in stud shank and variation with location along the span of composite girders is also presented. The interface slip is measured with a simple and innovative arrangement of dial gauges.

Present study is divided into three parts. The specimen design, fabrication, material and geometrical details, instrumentation and test setup and procedure are explained in first part. In the second part, experimental results under monotonic and cyclic loading are discussed. The analysis is carried out for maximum moment capacities of SCC girder specimens. Failure modes, summary and conclusions are discussed in last part.

2. Experimental investigation

Six specimens of high strength stud connected steel-concrete composite girders are tested to investigate the flexural behaviour. Three SCC girder specimens are tested under monotonic (quasi-static) loading and the other three under non reversal cyclic loading (loading and unloading, without reversal). Longitudinal section with geometrical details is shown in Fig. 1.

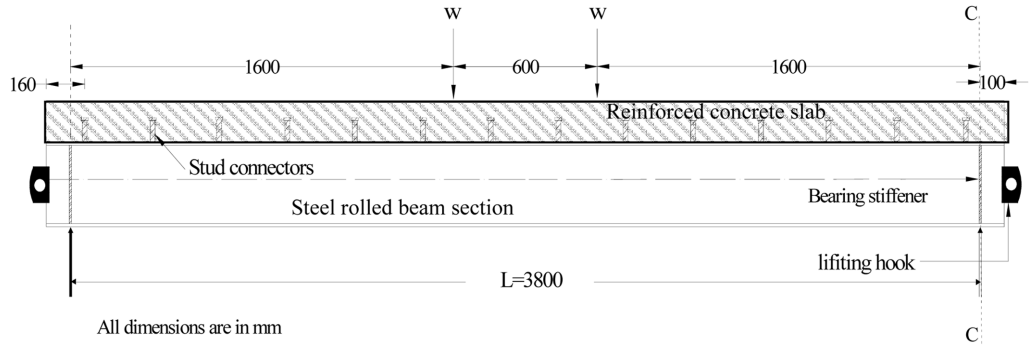

Fig. 1 Longitudinal section of SCC girder

2.1 Design, fabrication, casting and storage of girder specimens

2.1.1 Design basis

SCC girders specimens are designed using linear elastic analysis such that the yielding initiate from the bottom flange of steel beam. Yield load for SCC girder with full shear capacity is determined using linear elastic analysis as 360 kN and a factor of 1.5 is assumed for the estimation of maximum moment capacity of the girders.

This analysis required for the selection of hydraulic jack for loading the specimens. Therefore a hydraulic jack of 600 kN capacity was mounted on test frame. The reinforced concrete slab of specimens is designed based on Indian code of practice (IRC:22-1986), and some guidelines reported by Oehlers and Bradford (1995). Longitudinal and transverse reinforcement bars are provided in two layers with adequate spacing to avoid any premature splitting of concrete flange. Attention was also paid to keep adequate gap between reinforcement bars and the stud connectors for proper concreting in its vicinity. Thickness of concrete flange (150 mm) was decided based on 50 mm cover over the height (100 mm) of the flexible stud type shear connector as per the codes of practice.

Cross sectional details of stud connector and bearing stiffeners are shown in Fig. 2. The stiffeners were designed as per IRC:24-2000 to avoid shear failure of steel beam section, due to concentrated support reaction. Geometric dimensions of reinforced concrete flange and detailing of reinforcement bars are shown in Fig. 3. The detailed geometrical properties of concrete slab and steel beam are

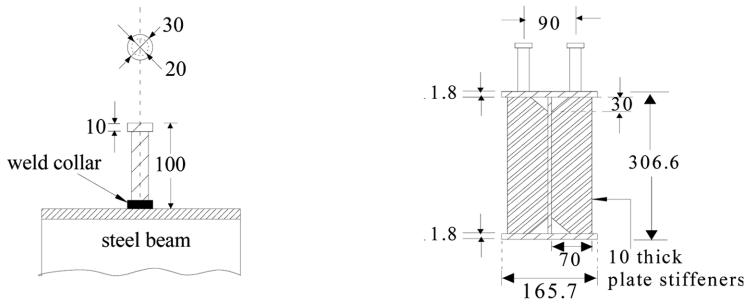

(a) Details of stud (section B) (b) Details of stiffener (section C-C)

Fig. 2 Sectional details

tabulated in Table 1.

Table 1 Geometrical and Material properties

	Details	Values
Geometrical		
Steel-concrete Composite girder used		
	Total length of girder specimens, mm	4000
	Clear span (between supports), mm	3800
	Shear span, mm	1600
CGS/CGC-1,2,3	Longitudinal stud spacing, mm	283, 313, 408
CGS/CGC-1,2,3	Total numbers of stud connectors (2 rows)	28,24,20
CGS/CGC-1,2,3	Number of stud connectors per row	14,12,10
Steel beam (IPM306@46.1 kg/m)		
	Area of cross section, mm^2	5806
	Total depth, mm	306.6
	Width of flanges, mm	165.7
	Thickness of flanges, mm	11.8
	Thickness of web, mm	6.7
Stud Connector		
	Diameter of shank, mm	20
	Diameter of head, mm	30
	Total length, mm	100
	Thickness of head, mm	10
Concrete slab		
	Width, mm	665
	Thickness, mm	150
	Transverse reinforcement, %	1.259
	Longitudinal reinforcement, %	0.916
Material		
Steel	Density, kg/m^3	7850
	Poisson's ratio	0.3
	Elastic modulus, MPa	210000
Structural	Yield strength, MPa	300
	Ultimate tensile strength, MPa	420
Studs connector	Yield strength, MPa	680
	Ultimate tensile strength, MPa	900
	Shear resistance (As per pushout test), kN	132
Reinforcement bar	Yield strength of reinforcing bar, MPa	415
	Ultimate tensile strength, MPa	550
Concrete	Density, kg/m^3	2500
	Elastic modulus, MPa	30000
	Poisson's ratio	0.2
	Average 28 days compressive strength of concrete (cylinder), MPa	36
	Average 28 days compressive strength of concrete (cube), MPa	41

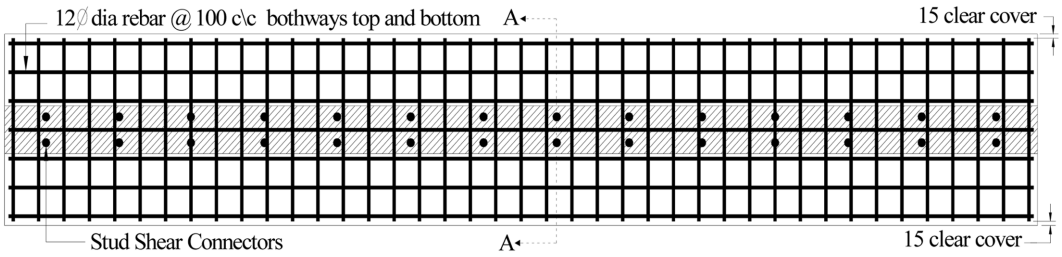

Fig. 3 Reinforcement in concrete slab

Width of concrete slab (665 mm) and size of rolled steel parallel flange beam (IPM 306 @ 46.1 kg/m weight) are kept same for all the specimens. The cross sectional details of steel concrete composite specimens are shown in Fig. 4. Similar specimens are fabricated for non-reversal cyclic loading and designated as CGC-1, CGC-2 and CGC-3 respectively. The number of shear connectors required for the full shear connection is determined as 14 per shear span, based on IRC: 22. Specimens are designated with suffix 1, 2, 3 for 100%, 85% and 75% shear capacity for equi-spaced stud connectors, in the shear span respectively.

2.2 Material specifications

2.2.1 Concrete

Ordinary Portland cement of 53 grade cement and crushed stone aggregate with maximum size of 12 mm and 20 mm were used in concrete. The concrete mix was designed as per guidelines of IS:10262 code and mixing was done in a conventional tilt type mixing machine, then poured into mould and compacted by means of needle vibrator. Concrete compressive strength is determined using 36 numbers of controlled cubes of size 150 mm × 150 mm × 150 mm. The average compressive strength after 28 days of the concrete was found 36 MPa.

2.2.2 Steel for beams

Steel beams having parallel flanges used in the specimen construction were standard hot-rolled steel shape IPM306 section, with a linear-weight of 46.1 kg/m. The ultimate and yield strengths of steel beam sections are 410 MPa and 300 MPa respectively.

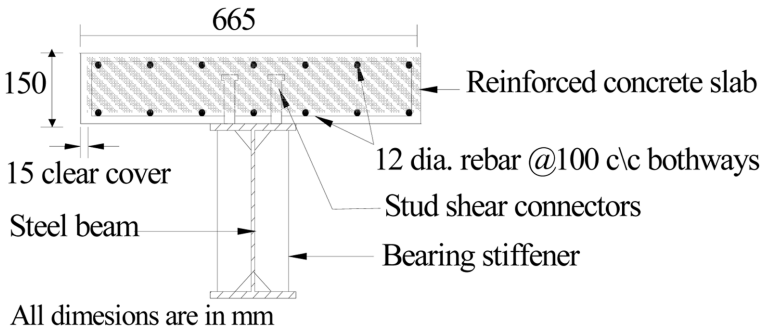

Fig. 4 Cross-sectional detail of the composite girder

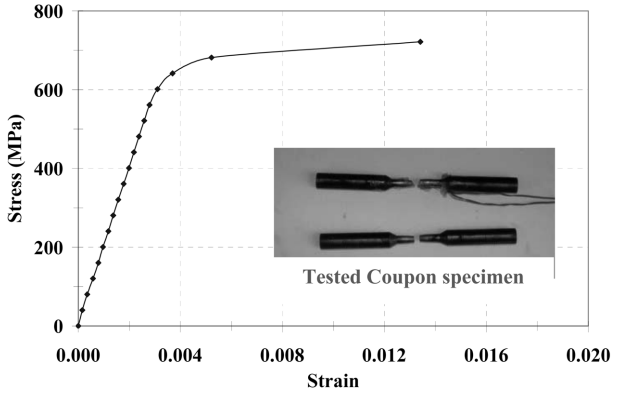

Fig. 5 Uniaxial tensile stress-strain behaviour of stud steel

2.2.3 Steel for studs

The steel used for studs was tested using standard Coupon tests (as per ASTM Procedures). It was found that the stud steel have ultimate strength 900 MPa, yield strength of 680 MPa and elongation as 14% as shown in Fig. 5. The average shear resistance of the stud connectors used in this study have been obtained as 132 kN from push out tests (Madheswaran *et al.* 2007).

2.2.4 Steel for reinforcement

Reinforcement in concrete slab was provided using high yield strength deformed bars of Fe-415 grade steel.

2.3 Fabrication of steel-concrete composite girder specimens

Stud connectors and plate bearing stiffeners were welded to the top flanges of the rolled steel beam (Fig. 6) in work shop using standard welding procedures (AWS). The primer coat was applied on the steel beams to avoid any adhesion effect and they were transported to casting yard. Then these steel beams were placed in position and wooden moulds were placed around them. Electrical strain gauges (TML strain gauges of 5mm gauge length and 120 Ohm electrical resistance) were pasted on the smoothened surface of stud shanks. Attention was paid to protect the strain gauges and lead wires from any damage during concreting. For this PVC sheaths were kept on wires and thin aluminium foil was wrapped around strain gauges see Fig. 7.

Motorized tilting type concrete mixer was used for the preparation of concrete near to casting yard. Concrete was poured in the specimens and compacted with needle vibrator as shown in Fig. 8. After 28 days of curing with saturated gunny bags at casting yard, the girders were shifted to laboratory for

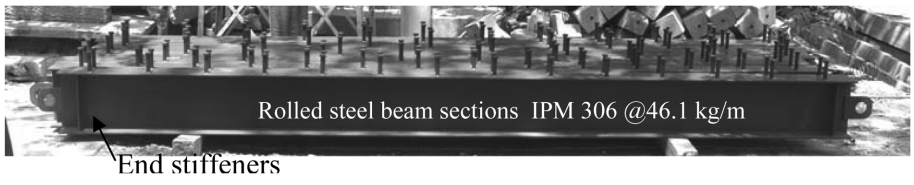

Fig. 6 Rolled steel beams with welded stud connectors and stiffeners

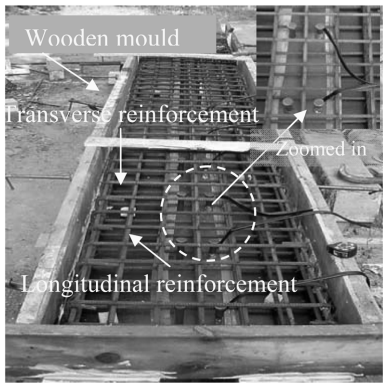

Fig. 7 Rolled steel beams with welded stud and reinforcement mesh

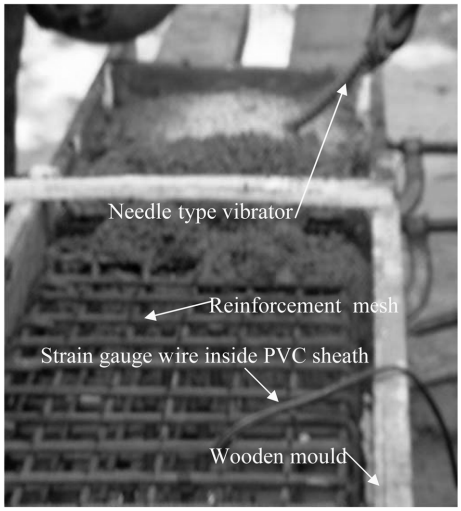

Fig. 8 Compaction of concrete using needle vibrator

testing.

2.4 Instrumentation

2.4.1 Dial gauges

Dial gauges are used for the measurement of vertical displacement at mid span and quarter span. Interface slips are also measured with the help of dial gauges mounted in horizontal position as shown in Fig. 9. Dial gauge bases were kept on fixed reference by means of a channel section kept along span. The dial gauge needle was kept parallel to the web in horizontal direction at the same level. Perspex plates were attached approximately 50 mm below the concrete bottom of RC slab with pieces of steel angle section and then pasted to steel flange and concrete slab at same section (See Fig. 9). The readings of both the dial gauges were noted for each load stage. Due to congestion problem, the measurements of interface slips were taken at alternate stud locations, along the span.

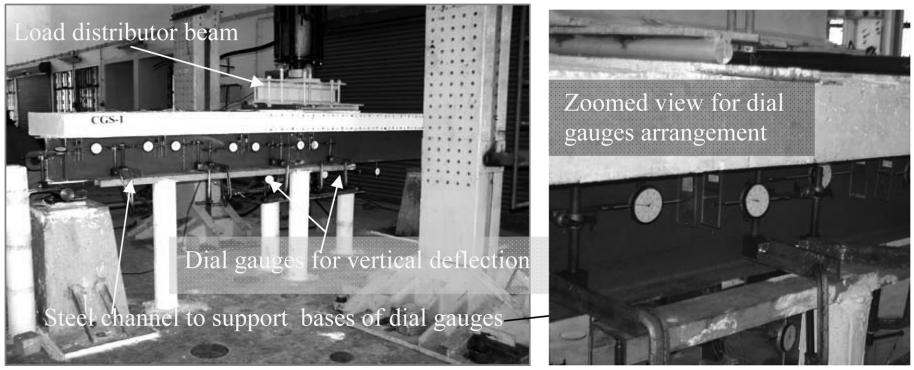

Fig. 9 Dial gauges arrangement for slip measurement

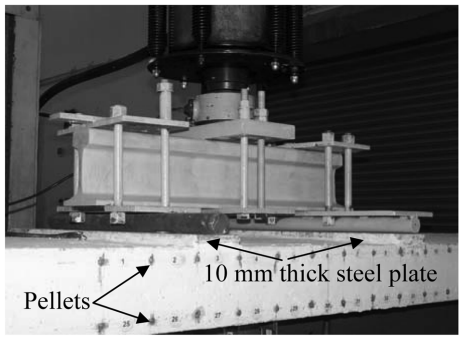

Fig. 10 Pellets fixed on concrete slab for strain measurement

Fig. 11 Strain measurement across depth of girder at mid span

2.4.2 Pellets and Strain gauges

The strains in longitudinal direction in concrete slab are measured using Pfender gauge. Pellets are fixed on concrete specimen at 100 mm c/c as shown in Fig. 10. Electrical strain gauges (TML strain gauges 5 mm/120 Ohm) are pasted across the depth of girder at mid span Fig. 11, to measure longitudinal strains profile. Strain gauges are pasted along height of studs on opposite sides of stud shanks as shown in Fig. 12, to measure longitudinal strains. The distribution and orientation of electrical

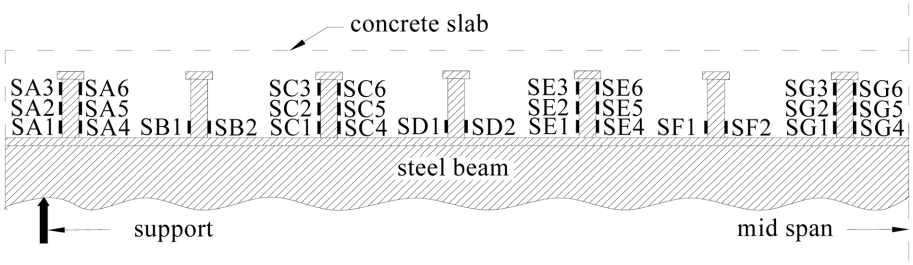

Fig. 12 Strain gauge locations for strains in studs of specimen CGS 1

strain gauges are in the longitudinal direction i.e. along the shank to obtain critical strain response. Strain gauges are pasted at three locations namely near bottom, middle and near top and a similar row on the opposite side shank face also (Fig. 12). The advantage of symmetry is taken by pasting the strain gauges only in one row of studs for half span.

For the specimens with suffix 2 and 3, pellets were pasted in middle third porion of RC slab only, as shown in Fig. 13. All embedded strain gauges as well as external gauges were connected to data logger for automatic recording as shown in Fig. 14.

2.5 Test Procedure

Three specimens (CGS-1, CGS-2, and CGS-3) are tested under quasi-static/monotonic loading, and the other three similar specimens (CGC-1, CGC-2, CGC-3) are tested under non-reversal cyclic loading. Steel-concrete composite girder specimens were placed over simple supports (one end roller and other rocker). A 600 kN capacity hydraulic actuator was used to apply the monotonic and cyclic loads. Loading was applied at two points near mid span, on the top of concrete slab through the distribution beam and two cross beams Fig. 9. To avoid any concentrated contact forces at load points, two 10 mm thick steel plates are kept above the concrete top surface across full width of slab below loading beam as shown in Fig. 10.

Initially the 25% of the load was applied and then specimen was unloaded. This is recommended by various codes of practices and guidelines, for checking the test set up. Then loading was applied in the

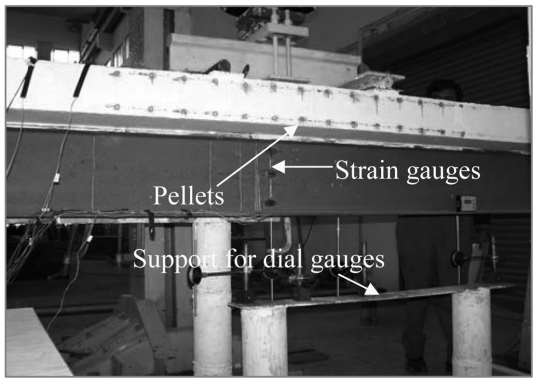

Fig. 13 Dial gauges, strain gauges and pellets in specimen 2 and 3

Fig. 14 Strain recording using data logger

increments of 50 kN for monotonic load test while non-reversal cyclic test was carried out based on yield deflection and 1, 3 and 5 times of the yield deflection was applied in displacement controlled manner. The time taken to complete one specimen testing took about 4 hours. The manual recording of the interface slip and Pfender gauges readings took at least 15~20 minutes time after each increment of the load which is the main reason for testing duration.

3. Experimental Results and Discussions

3.1 Monotonic

3.1.1 Load- deflection behaviour

Comparison of load-deflection behaviour under monotonic loading for three SCC girder specimens is shown in Fig. 15. Load-deflection behaviour is idealized as trilinear curve, elastic before yield (O-A), yield to peak (A-B1) and post peak region is B1-F1). Points with suffix 2 and 3 are corresponding to specimen 2 and 3 respectively. Load at various stages namely yield (P_y), ultimate (P_u) and failure (P_f) are depicted in Fig. 15 and compared in Table 2. In addition to the loads, displacements corresponding to yield, peak and failure denoted as δ_y, δ_u and δ_f respectively are also provided in Table 2. Specimens showed linear elastic behaviour upto about 40% of maximum load capacity. All the three SCC girder specimens under monotonic loading attained the maximum load carrying capacity, and failed showing large plastic rotation. The peak load capacity was marginally higher for CGS-1 as compared to other specimens with lesser stud connector density. Maximum failure displacement was recorded for CGS-1, slightly less for CGS-2, and further lesser displacement was obtained for CGS-3.

The ductility ratio δ_f/δ_u defined as failure deformation to ultimate deformation was obtained (using Fig. 15) as 3.4, 4.5 and 3.3 for CGS-1, 2 and 3 respectively. All the specimens have exhibited very good ductility which is advantageous to absorb more energy before failure. Although ultimate loads obtained experimentally are almost same for specimen CGS-2 (495 kN) and CGS-3 (480 kN), yet ductility differs (see Table 2) this may be due to the effect of force distribution among stud connectors.

Table 2 shows that the failure loads are approximately equal to the predicted yield load for SCC girders with full shear connection. This is true because once the concrete slab reaches crushing at the top face there is only steel beam which resists the load. It can also be seen that specimens have

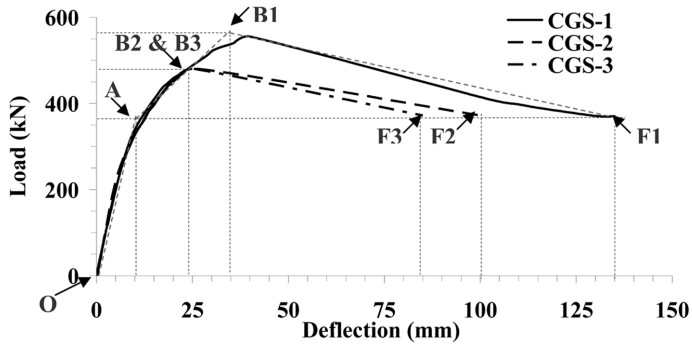

Fig. 15 Load-deflection at mid span under monotonic loading

Table 2 Ductility ratio of SCC girders under monotonic loading

Specimen	Load, kN			Displacement, mm			Ductility		
	P_y	P_u	P_f	δ_y	δ_u	δ_f	δ_u/δ_y	δ_f/δ_u	δ_f/δ_y
CGS-1	360	555	370	12.2	40.1	135.0	3.3	3.4	11.1
CGS-2	360	495	372	12.3	26.8	100.0	2.2	4.5	8.1
CGS-3	360	480	372	11.3	25.5	85.0	2.3	3.3	7.6

exhibited very good ductility at failure varying as 11.1, 8.1 and 7.6 for CGS-1, 2 and 3 respectively. This indicates the advantage of SCC construction as compared with RCC and steel. All the three specimens have showed ductility at failure more than 7, however the reduction in degree of shear connection reduces the ductility of SCC girders.

3.1.2 Interface Slip Behaviour

The experimental values of interface slip corresponding to load 360 kN (yield load) and 480 kN (near maximum load) are plotted in Fig. 16(a) and Fig. 16(b). Theoretically maximum interface slip occurs near the end of the simply supported beam, but due to support influence little reduction in slip has been observed under the experimental conditions. Similar variation due to distribution of stud near support has also been reported (Ayoub 2005). It is observed that the slip increases with decreasing degree of

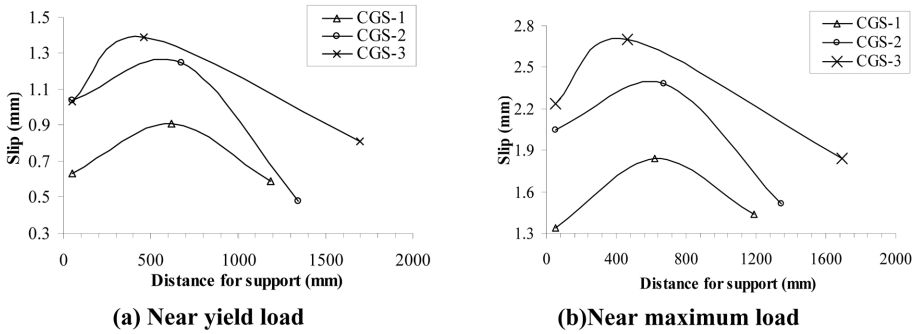

Fig. 16 Slip at steel-concrete interface

shear connection. The maximum interface slip for CGS-1 was recorded as 3.56 mm at section near to the support.

3.1.3 Strain Response

3.1.3.1 Steel Beam

Longitudinal strain variation at mid span along the height of composite girders is shown in Figs. 17 (a) for specimens 1, 2 and 3. It is inferred from the variations of the longitudinal strain that full steel section is utilized in tension which shows the advantage of composite construction. It is noted that initially for lower load (i.e., 25% of maximum load), full shear interaction occurs (i.e., no interface slip), but for higher loads a step change in strain values observed at the interface. This step change in strains results into the interface slip (due to strain incompatibility), which is usually referred to partial shear interaction.

Longitudinal strains at mid span in the rolled steel section for specimens 1, 2, and 3 are shown Figs. 17(b). It can be seen that the rolled steel sections in all the specimens at mid span have nearly zero strain at top and maximum tensile strain at bottom. This shows that due to SCC construction almost entire steel section is subjected to tension for which it is basically strong. Yielding of bottom flange at

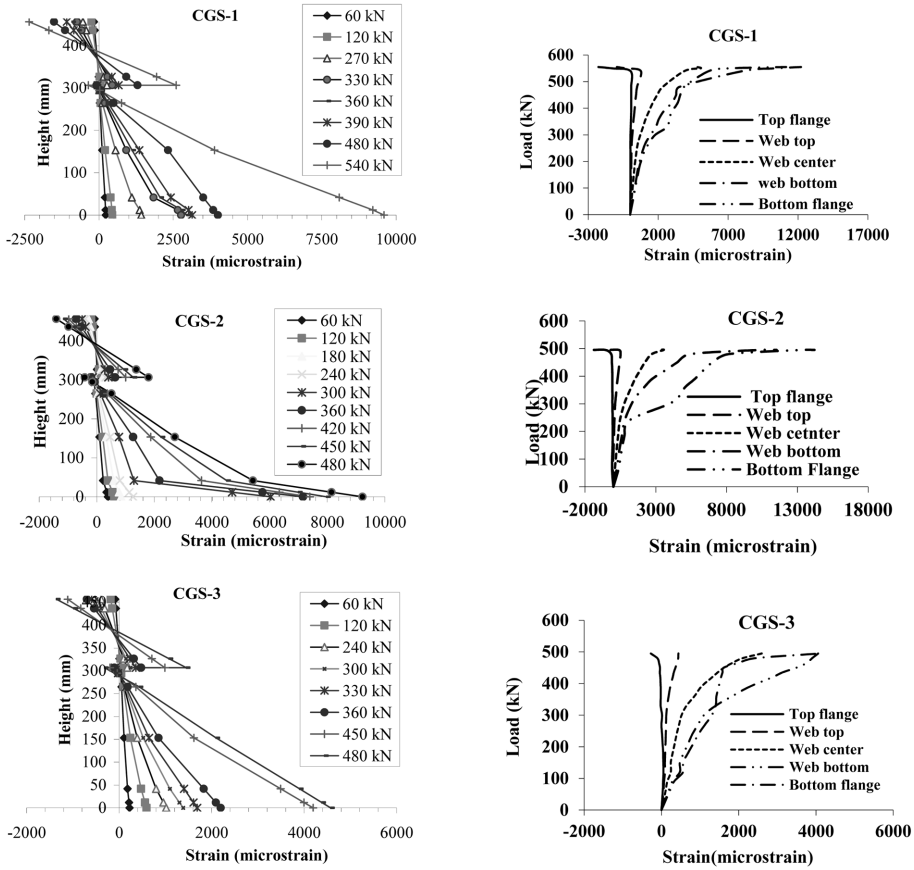

(a) Variation along height of girder **(b) In steel beam section**

Fig. 17 Longitudinal strain response at mid span

the quarter span was observed at about maximum load. Strains at various levels in web were recorded and it was observed that the web strains are tensile in nature and magnitude was found to increase from top to bottom flange. This is unlike non-composite construction where half of the steel section is subjected to compressive stress due to which full strength of rolled steel section can not be utilized.

3.1.3.2 Concrete Slab

Concrete is considered to reach its maximum compressive stress at a strain value between 0.002 and 0.003 and at higher stress it gets crushed (CEB 1996). Strain in concrete slab is measured by both electrical resistance type strain gauge and Pfender gauge. Maximum tensile strains on bottom face of reinforced concrete slab at mid span were recorded as 566 με and 1970 με corresponding to yield load and maximum load as shown in Fig. 18(a). At quarter span tensile strain are recorded as 203 με and 1000 με at yield load and maximum load respectively as shown in Fig. 18(a). This indicates that longitudinal stress decreases as we move away from the mid span. Strains are found dominated in middle one-third portion of full length specifically near and in-between loading points. Strains beyond on either side of middle one-third portion are found insignificant as shown in Figs. 18(b) and 18(c). Tensile strain measured below left load point is 700 με at yield load and 4320 με at ultimate load. This clearly indicates that the steel reinforcement in concrete slab has also yielded. Thus the section has been fully utilized. The compressive strain is recorded as 805 με at yield load and 2060 με at ultimate load (crushing of concrete).

Crack pattern observed in the central region was similar to a reinforced concrete specimen subjected to axial load and flexure. The depth of cracking was maximum in the constant bending zone and decreased rather rapidly in the flexure-shear zone.

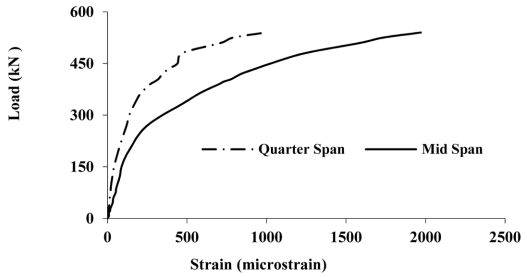

(a) Longitudinal strain in RC Slab bottom face

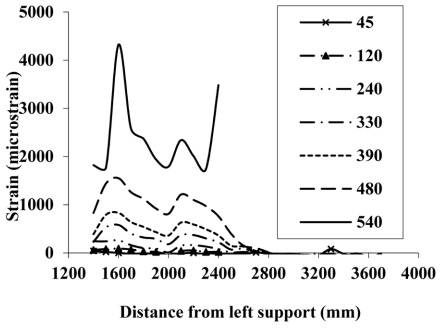

(b) Tensile strain at bottom of RC slab

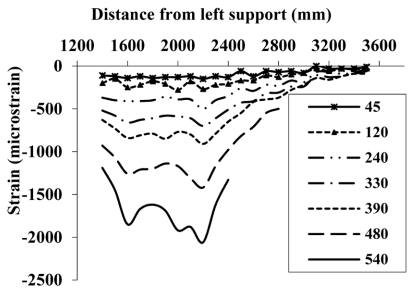

(c) Compressive strain at top of RC slab

Fig. 18 Longitudinal strain response in concrete slab at various loads

3.1.3.3 Studs

It is found that the stud connectors in composite girders undergo a varying degree of flexure, and tension depending upon the location with respect to supports. The analysis of strain data of stud shanks at various locations reveals the inner mechanism of stud deformation. It is observed that strain along the stud shank varies along the length of stud as well as along the span of the SCC composite girder. Further the nature of deformation tends to undergo deformation with double curvature. It can be seen from Fig. 19 that the strain sign changes at opposite face. This indicates rotation, bending and elongation in the stud shank. Magnitude of strains in shank of studs near support is found to be higher than those near to the mid span. This information may be useful in the design of SCC structures to distribute more number of connectors near supports to control interface slip in better way. It is interesting to note that the strains at the top and bottom sections of shank depict similar nature on diagonally opposite face (refer Fig. 20). Hence it can be inferred from the experimental data that stud connector deforms in double curvature.

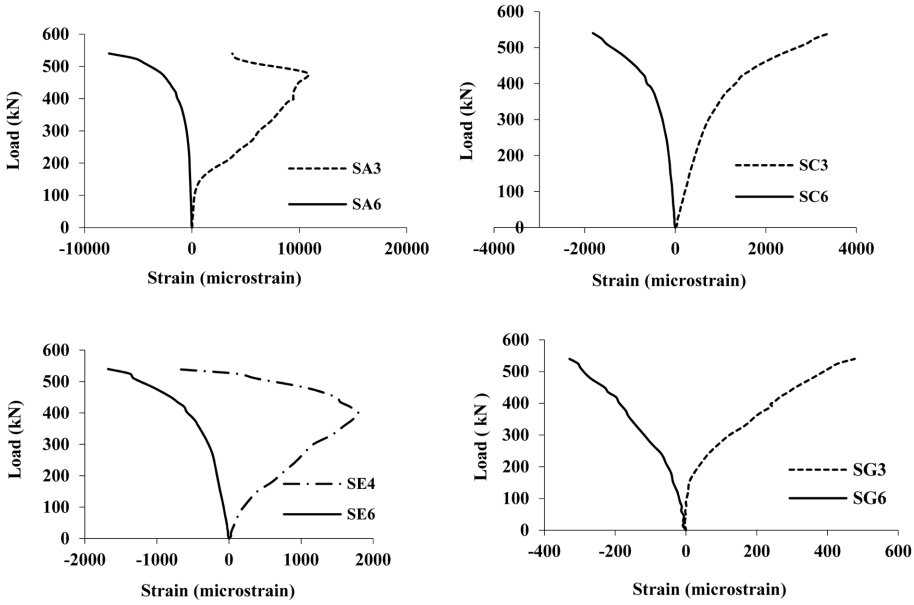

Fig. 19 Strain developed in stud shank of specimen CGS-1

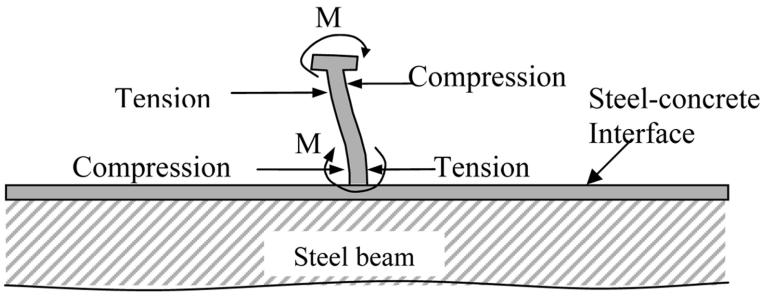

Fig. 20 Deformation of stud connector

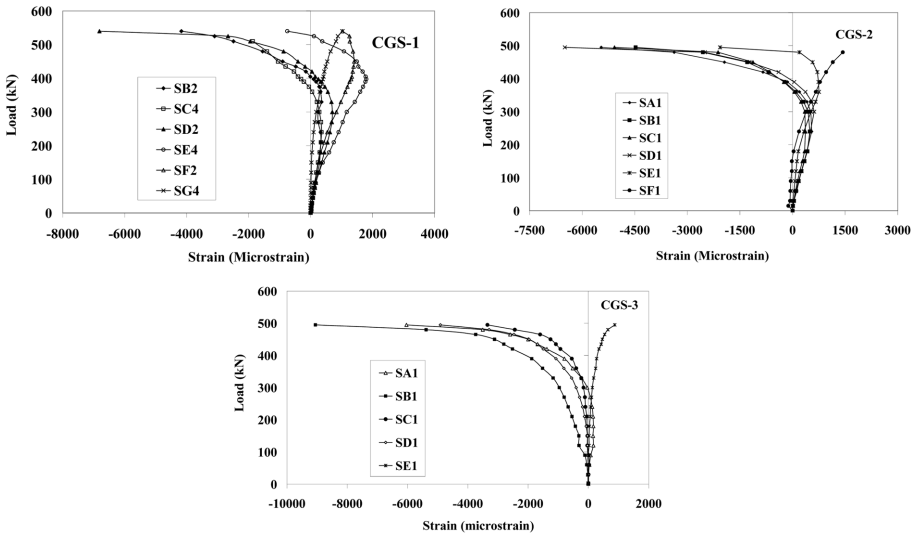

Fig. 21 Strain variation in stud shanks along span

It is also observed that the distribution of the strains in shank varies depending on the load on the girder and position of the stud with respect to support or mid span. Fig. 20 shows deformation of stud due to flexural behaviour of stud.

Fig. 21 shows the strain variation along the span in the stud shanks near the bottom. It is observed that there is a change in strain sign from tension to compression at a load value about 60~80% of maximum load value. In addition to that, the studs near to the support exhibit higher magnitude of strain than those near to mid span.

3.2 Non-reversal cyclic test results

The cyclic tests were also carried out by loading and unloading in displacement controlled mode. Each displacement increment is based on yield displacement and consists of three loading and unloading cycles. The comparison of load deflection for cyclic and monotonic loads is shown in Fig. 22. It can be seen that load-deflection curves of SCC girders for monotonic loading superimposed well over that for the cyclic loading. Unlike normal reinforced concrete girders, the cyclic loading is found to make no significant change in behaviour. Hence it can be stated that cyclic load did not deteriorate the flexural capacity of the section, particularly with respect to stiffness. It can be seen from Table 3 that all three section show very good ductility which can be of much importance for seismic and blast resistant designs.

4. Modes of failure

All the three of steel-concrete composite girder specimens exhibited similar flexural failure modes with fracturing of shear connectors, characterized by the crushing of concrete slab in the pure bending region. Crack patterns were dominated by flexural cracks, which spread throughout the width of slab.

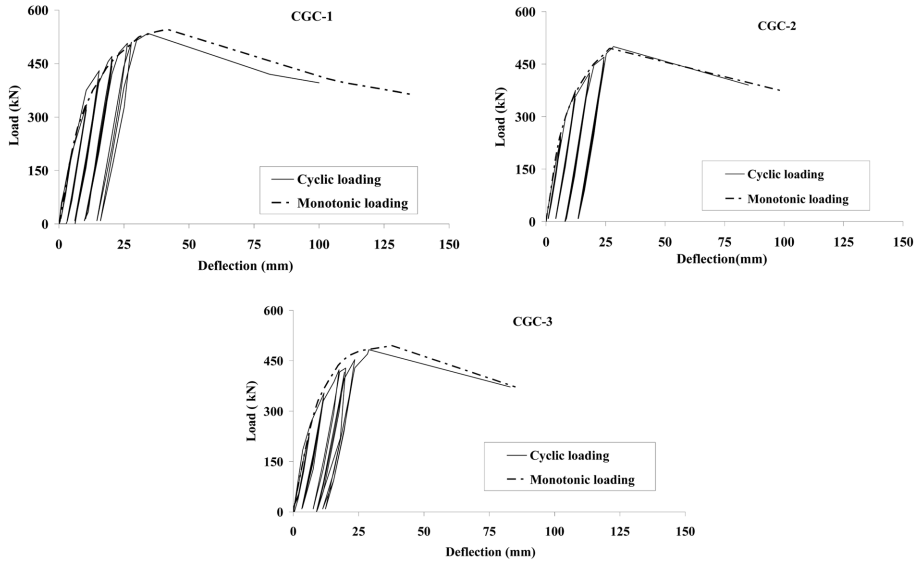

Fig. 22 Load-deflection under cyclic and monotonic loading

Table 3 Ductility of SCC girders under cyclic loading

Specimen	Load, kN			Displacement, mm			Ductility		
	P_y	P_u	P_f	δ_y	δ_u	δ_f	δ_u / δ_y	δ_f / δ_u	δ_f / δ_y
CGC-1	360	535	396	10.6	34.2	100	3.2	2.9	9.4
CGC-2	360	500	390	11.9	28.4	85	2.4	3.0	7.2
CGC-3	360	483	372	11.8	28.9	83	2.5	2.9	7.0

The yielding was observed at the bottom flange of the rolled steel beam and the flexural cracks in concrete slab started appearing Fig. 23(a) and kept growing till crushing at top of the concrete slab near load points. The failure occurred by fracture of studs with a loud noise, near the roller end supports, and then crushing of concrete at top near load point is observed. The local buckling of top flange of steel beam under the left side load point also observed when the specimen failed, as shown in Fig. 23(b). One possible reason for this local buckling in the region of maximum compressive stress developed in top flange due to shifting of neutral axis down ward after RC slab get crushed at top. Other possibility may be due to the influence of spacing of the studs and top flange thickness of steel beam due to variation in constrained length of flange as reported by Uy and Bradford (1996). It is felt that the local buckling of the top flange in the present case is due to b/t ratio, where 'b' is the width of overhang beyond the web. Wide flange sections with thin flanges are prone to the above buckling. May be provision of a lip at ends of the top flange over the maximum bending moment region would help to avoid the above local buckling. The above recommendation is based on the profile of the buckled top flange as observed in tests.

4.1 Maximum flexural capacity

Maximum moment capacities of the specimens were determined using elastic-plastic analysis and the

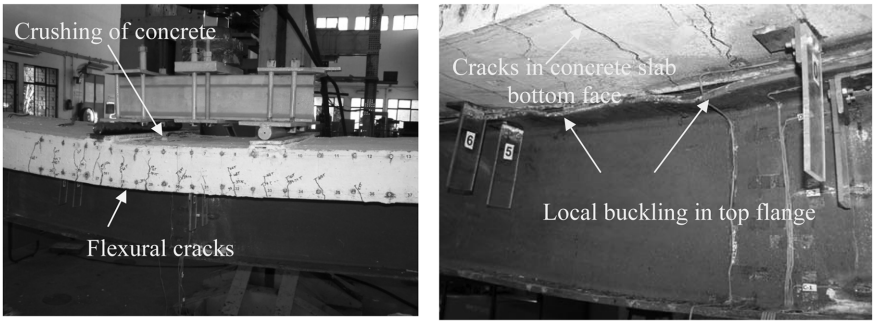

(a) Flexural cracks in RC slab at failure (b) Buckling of top flange of steel beam at failure load

Fig. 23 Failure modes in tested SCC girder specimens

results are shown in Table 4. It was assumed that the stress level corresponding to maximum strain values as recorded from flexural tests were lesser than the ultimate strength of steel (410 MPa). The reason for this assumption was, for instance, no rupture was occurred in the steel beam section during tests till failure load. Considering this stress value at extreme steel fiber was obtained iteratively based on experimental strain value with respect to maximum strain recorded (i.e., 9596 micro strain for CGS-1 specimen). The ultimate tensile strength was determined such that the applied bending moment (experimental) matched with analytical bending moment capacity of SCC girder. Later same ultimate tensile stress was used for other two specimens and linearly interpolated based on the strain level. Steel beam portion near to the top flange is neglected as it is closer to neutral axis and does not contribute much towards the flexural strength of the composite girder sections. Bending moment capacity is obtained by taking moment of all the forces as depicted in Fig. 24, about interface. Compression is denoted as 'C' and tension with letter 'T' along with proper suffixes for concrete and steel portions.

Efficiency factor indicated in Table 4, is the effectiveness of high strength stud connectors in resisting interface forces both axial and transverse. Efficiency factor for the high strength stud is obtained from the analysis is about 0.8, which corroborates with the recommendations of Eurocode 4. It means that the value of shear strength of a stud obtained from push-out test can be used in the design of SCC girders with a multiplication factor of 0.8.

Table 4 Comparison of experimental and analytical flexural capacities

	CGS-1	CGS-2	CGS-3	Unit
Effective number of stud in shear span	12	10	8	
Strain at bottom flange (experimental)	9596	5900	4574	Microstrain
Ultimate stress at bottom of flange (based on strain)	380	343.5	330.4	MPa
Average stress for yielded web portion	340	321.7	315.2	MPa
Stud force (neglecting studs in pure bending zone), P_{stud}	1584.0	1320.0	1056.0	kN
Total force in steel beam, P_{steel}	1262.8	1120.4	1043.4	kN
Efficiency factor	0.80	0.85	0.99	
Applied bending moment (experimental)	450.2	402.2	390.2	kNm
Moment of resistance of SCC girder (analytical)	450.3	409.3	389.7	kNm

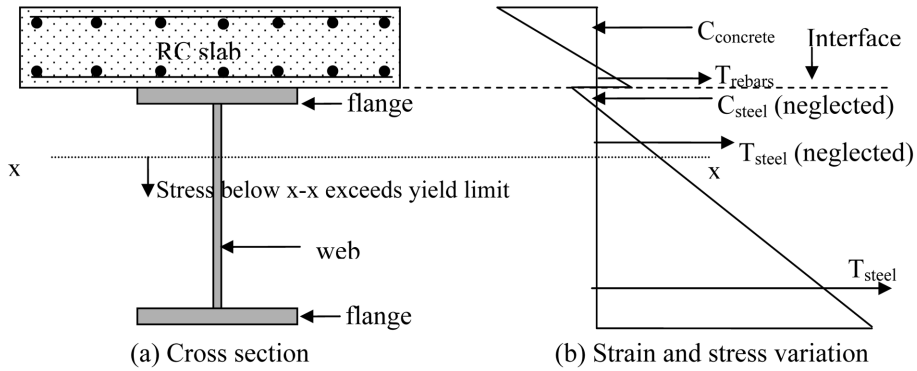

Fig. 24 Typical stress distribution in SCC girder specimen used in analysis

5. Conclusions

Experimental study on steel-concrete composite girders has been presented. The reinforced concrete slab was designed such that the premature splitting does not occur in concrete slab. Yielding of the steel top flange was observed prior to flexural cracks in the bottom of concrete slab. All the specimens have failed in flexure characterised by fracture in stud connectors with loud noise. A simple and innovative method was used for the measurement of interface slips between concrete slab and top flange steel beam. Following conclusions are drawn from the study:

It was found that due to reduction in stud shear connector density, the ultimate moment of resistance as well as ductility get reduced for HSS stud connected SCC girder.

Maximum interface slip between steel flange and RC slab for SCC girder specimen having full shear capacity was obtained 3.56 mm near support. Variation of slip along span shows reduction towards mid span.

Load-deflection envelope for non-reversal cyclic tests compared well with the monotonic test results. There was not much deviation in flexural behaviours between these two types of loadings.

Strain in stud shank indicated inflexion which means that the studs deform with double curvature. However depending upon location of stud, the strain magnitude varies.

The experiments exhibited that the degree of shear restraint provided by the stud affects the ultimate load capacity.

The most significant improvement in terms of structural behaviour relates the stiffness at working stage. Assuming 'peak load/1.5' can be approximated as the working load; the deflection at this stage in all the specimens was only about 8 mm, approximately span divided by 500. Ductility as defined by δ_f/δ_y is found significantly high about 11 and 9 under monotonic and cyclic loading respectively for section having full shear capacity, which shows utility of such SCC girders for better energy absorption.

Load reduction at failure is less than 25% compared to peak load stage. Response reduction factors hence would be significantly high for seismic and blast resistant design.

The efficiency factor was obtained as 0.8 for HSS stud connected SCC composite girders. This corroborates well with the existing Eurocode 4 guidelines.

Spacing of the studs and top flange thickness of steel beam has influence on the local flange buckling. For this guidelines may be provided so that rolled steel beam sections can be selected to avoid the buckling of the constrained flange. One of the recommendations could be limiting the ultimate load

capacity to 1.5 times the plastic moment capacity of the section such that the post peak load reduction is kept within limits.

Acknowledgement

The authors wish to acknowledge the support rendered by staff of Advanced Material laboratory and structural testing laboratory at CSIR-SERC, in conducting the experiments. The first author would like to thank Dr. J. Rajasankar for the encouragement and motivation in writing this paper. This paper is being published with the kind permission of Director, CSIR - Structural Engineering Research Centre, Chennai, (INDIA).

References

AWS. (2006), American welding society, Structural welding code.

Bouazaoui, L. Perrenot, G., Delmas, Y. and Li, A. (2007), "Experimental study of bonded steel concrete composite structures", *J. Constr. Steel Res.*, **63**(9), 1268-1278.

CEB. (1996), RC elements under cyclic loading, state of the art report, Comite Euro-International DU Beton, Thomas Telford, 1996.

Chapman, J.C. and Balakrishnan, S. (1964), "Experiments on composite beams", *Struct. Eng.*, **42**(11), 369-383.

DD ENV 1994-1-1, Eurocode 4, Design of composite steel and concrete structures- Part 1.1: General rules and rules for building, London: British Standards Institution.

IRC: 22-1986, "Standard specification and code of practice for road bridges, section VI, (Composite Construction)", The Indian road congress, New Delhi.

IRC: 24-2000, "Standard specification and code of practice for road bridges, (Composite Construction)", The Indian road congress, New Delhi.

IS 10262-1982. IS recommended guidelines for mix design. Bureau of Indian Standards.

Jasim, N.A. (1999), "Deflections of partially composite beams with linear connector density", *J. Constr. Steel Res.*, **49**(3), 241-254.

Johnson, R.P. and Oehlers, D.J. (1981), "Analysis and design for longitudinal shear in composite T-beams", *Proceedings of Institution of Engineers*, London, Part 2, vol. 71, December, 989-1021.

Jurkiewiez, B. and Hottier, J.M. (2005), "Static behaviour of a steel-concrete composite beam with an innovative horizontal connection", *J. Constr. Steel Res.*, **61**(9), 1286-1300.

Jurkiewiez, B. (2009), "Static and cyclic behaviour shear connections", *J. Constr. Steel Res.*, **65**(12), 2207-2216.

Jurkiewiez, B. and Braymand, S. (2007), "Experimental study of a pre-cracked steel–concrete composite beam", *J. Constr. Steel Res.*, **63**(1), 135-144.

Lam, D. and El-Lobody, E. (2005), "Behaviour of headed stud shear connectors in composite beam", *Journal of Struct. Eng.*, **131**(1), 96-107.

Liang, Q.Q., Uy, B., Bradford, M.A. and Ronagh, H.R. (2004), "Ultimate strength of continuous composite beams in combined bending and shear", **60**(8), 1109-1128.

Madheswaran, C.K., Natarajan, K. and Prakash, A. (2007), "Strength of shear connectors in steel concrete composite beams", *Journal of Institution of Engineers (India)*, **88**(8), pp 14-20.

Mirza, O. and Uy, B. (2009), "Effects of steel fibre reinforcement on the behaviour of headed stud shear connectors for composite steel-concrete beams", *Advanced Steel Construction*, **5**(1), 72-95.

Nie, J. and Cai, C.S. (2003), "Steel-Concrete Composite Beams Considering Shear Slip Effects" *J. Struct. Eng.*, **129**(4), 495-506.

Nie, J., Cai, C.S., Wu, H. and Fan, J.S. (2006), "Experimental and theoretical study of steel-concrete composite beams with openings in concrete flange", *Eng. Struct.*, **28**(7), 992-1000.

Nie, J., Xiao, Y., Tan, Y. and Wang, H. (2004), "Experimental Studies on Behaviour of Composite Steel High

Strength Concrete Beams", *ACI Structural Journal*, **101**(2), 245-251.
Oehlers, D.J. and Coughlan, C.G. (1986), "The shear stiffness of stud shear connections in composite beams", *J. Constr. Steel Res.*, **6**(4), 273-284.
Oehlers, D.J. and Johnson, R.P. (1987),"The strength of stud shear connections in composite beams", *Structural*, **65B**(2), 44-48.
Oehlers, D.J. and Bradford, M.A. (1995), Composite steel and concrete structural members: Fundamental Behaviour, first edition, Pergamon Press, Oxford.
Oehlers, D.J., Nguyen, N.T., Ahmed, M. and Bradford, M.A. (1997), "Partial Interaction in Composite Steel and Concrete Beams with Full Shear Connection", *J. Constr. Steel Res.*, **41**(2-3), 235-248.
Oven, V.A., Burgess, I.W., Plank, R.J. and Abdul, W.A.A. (1997), "An analytical model for the analysis of composite beam with partial interaction", *Comput. Struct.*, **62**(3), 493-504.
Shim, C.S., Lee, P.G. and Yoon, T.Y. (2004), "Static Behaviour of large shear stud connectors", *Eng. Struct.*, **26**(12), 1853-1860.
Slutter, R.G. and Driscoll, G.C. (1965), "Flexural strength of steel-concrete composite beam", *Journal of Structural Division*, ASCE, **91**(ST2), 71-99.
Uy, B. and Bradford, M.A. (1996), "Elastic local buckling of steel plates in composite steel-concrete members", *Eng. Struct.*, **18**(3), 193-200.
Zhao, G. and Li, A. (2008), "Numerical study of a bonded steel and concrete composite beam", *Comput. Struct.*, **86**(19-20), 1830-1838.

CC